Toxicology Reports 14 (2025) 101857

Contents lists available at ScienceDirect

Toxicology Reports

journal homepage: www.elsevier.com/locate/toxrep

Natural hemozoin and β-hematin induce tissue damage and apoptosis in human placental explants

Carolina López-Guzmán [a,*], Julieth Herrera [a,b,c], Julián Zapata [c], Adriana Pabón [a], Urlike Kemmerling Weis [d], Ana María Vásquez [a,e,**]

[a] Grupo Malaria, Universidad de Antioquia, Colombia
[b] Grupo de Estado Sólido, Universidad de Antioquia, Colombia
[c] Laboratorio Análisis de Residuos, Universidad de Antioquia, Colombia
[d] Laboratorio de Mecanismos de infección parasitaria, Universidad de Chile, Chile
[e] Escuela de Microbiología, Universidad de Antioquia, Colombia

ARTICLE INFO

Handling Editor: Prof. L.H. Lash

Keywords:
Hemozoin
β-hematin
Malaria
Placenta
Plasmodium
Falciparum

ABSTRACT

Hemozoin (HZ) is a waste product of hemoglobin digestion by *Plasmodium* and has been implicated in several pathological processes, including inflammation, oxidative stress, endothelial dysfunction, and immune dysregulation. Studying the effects of HZ on the human placenta is essential to understanding the impact of malaria infection during pregnancy. The present study explored the impact of HZ produced by *Plasmodium* and β-hematin, referred to here as natural HZ (nHZ) and synthetic HZ (sHZ), respectively, on human placental explants exposed *in vitro*.

Methodology: nHZ was derived from *Plasmodium falciparum* cultures and isolated using magnetic MACS® Separation Columns (Miltenyi Biotec, Auburn, CA) [1]. sHZ was synthesized from hemin closure in an aqueous solution. Both nHZ and sHZ were characterized by infrared spectroscopy and scanning electron microscopy. Human placental explants (HPE) were exposed to 5 and 10 μg/mL of nHZ and sHZ for 24 h, and tissue integrity was studied using histological and immunohistochemical techniques.

Results: The studies have demonstrated that the exposition of both the nHZ and sHZ to placental tissue are comparable and cause effects in increased STB detachment, dysregulation of collagen distribution in the villous stroma, and increase in the frequency of cell apoptosis. This contributes to the understanding of the pathophysiology of malaria in pregnancy using synthetic products such as β-hematin.

1. Introduction

Malaria is a parasitic disease that affects millions of people every year and causes more than 608,000 deaths globally in 2022 [2]. Malaria is caused by parasites of the *Plasmodium* genus that infect and multiply in red blood cells (RBCs). These parasites use hemoglobin as a source of nutrients and produce hemozoin (HZ), also known as malaria pigment, an insoluble, undegradable, and iron-containing waste product of hemoglobin (Hb) digestion [3,4].

The parasites ingest Hb from the cytoplasm of RBC through endocytosis via the cytostome. In the digestive vacuole (DV), an acidic lysosome-like organelle induces the proteolysis of Hb, releasing heme-containing ferrous iron ($Fe2^{+}$), which instantaneously oxidizes to highly toxic heme-containing ferric iron ($Fe3^{+}$), harmful to the parasite [5]. The parasite modifies the heme released by Hb catabolism, converting dimers of hematin into the inert crystals of HZ to reduce the toxic effects of free heme. This process is necessary for the survival of *Plasmodium* parasites. Drugs that interfere with crystal formation have been highly effective in treating malaria [5,6].

HZ is released during schizogony, and after RBC rupture, the concentration of HZ in the bloodstream may be as high as 100 μg/mL [7], quickly removed from circulation by the liver and spleen. There are conflicting reports regarding whether HZ contributes to the systemic inflammatory responses during malaria infection. These discrepancies may be due to differences in experimental setups, such as the use of natural (nHZ) or β-hematin-synthetic HZ (sHZ), variation of methods

* Corresponding author.
** Corresponding author at: Grupo Malaria, Universidad de Antioquia, Colombia.
E-mail addresses: carolina.lopezg@udea.edu.co (C. López-Guzmán), amaria.vasquez@udea.edu.co (A.M. Vásquez).

https://doi.org/10.1016/j.toxrep.2024.101857
Received 14 October 2024; Received in revised form 29 November 2024; Accepted 7 December 2024
Available online 8 December 2024

used to isolate nHZ, use of varying concentrations of HZ preparations, and technical limitations of HZ generation and isolation methods [4,8].

As the infection progresses, HZ can accumulate and be observed within several organs, including the spleen, liver, bone marrow, lungs, brain, and placenta. HZ has both pro- and anti-inflammatory properties, and its accumulation in tissues has been correlated with disease severity [4,8]. Furthermore, since HZ is resistant to degradation, the duration of its pathological effects remains unknown and could extend beyond parasite clearance [4].

Several biomolecules have been described as interacting with HZ, such as lipids, parasitic DNA, fibrinogen, and red blood cell membranes. However, it is unknown whether the immune activation induced by HZ is due to the HZ itself or the various biomolecules binding to the molecule's surface [9]. A significant effect previously described of HZ is its role as a direct inducer of apoptosis in malaria pathogenesis, without any host or parasitic contamination (leukocytes, platelets, parasite DNA) [10]. Data support that HZ can directly contribute to the induction of apoptosis in neurons and astrocytes in cases of cerebral malaria [10]. In the same way, additional components to HZ, such as the heme group released during the cellular lysis of the erythrocytic cycle of *Plasmodium*, have been described to not only significantly induce cellular apoptosis in trophoblast cells but also hinder the fusion of these cells, which would be related to the malfunction of placental tissue during gestation [11].

Accumulation of HZ in human tissues has been frequently studied in the placenta of pregnant women with malaria, as the organ is accessible after delivery. The presence of HZ, infected RBCs, and inflammatory immune cells from the mother contribute to adverse effects of malaria during pregnancy, such as low birth weight (LBW), intrauterine growth retardation (IUGR), preterm delivery (PT) and miscarriage [12,13]. Histological observations of the placenta have shown that HZ accumulates in maternal phagocytic cells, fibrin deposits within the maternal blood space, and the chorionic villi. The presence of HZ is often used to determine the stage of the placental infection [13]. Acute active infections refer to infected RBCs in the tissue, while chronic active infections indicate the presence of both infected RBCs and HZ. Due to the ability of HZ to persist in the tissue even after infections have been resolved, past placental infections refer to the presence of only HZ deposits [14].

The syncytiotrophoblast (STB) that cover placental villi respond actively to HZ by producing inflammatory mediators such as cytokines and chemokines and inducing the activation of and chemotaxis of peripheral blood mononuclear cells toward syncytium [15]. Since the inflammatory response is associated with adverse effects such as LBW and IUGR [16–18]. Despite the advances described so far in the study of HZ, there is limited information about the direct impact of HZ on placental tissue due to several challenges. A significant difficulty lies in distinguishing, *in vivo*, the effects of the entire parasite from those of isolated HZ, as they interact in complex ways during infection. Moreover, investigating the direct effects of HZ on placental tissue accounting for the human cells present in the intervillous space poses significant methodological challenges. Furthermore, few studies compare the impact of nHZ, which may include parasite components, with sHZ, which lacks such components, on human placental tissue. This gap in research limits the understanding of how HZ directly affects placental structure and function. It is plausible to suggest that the accumulation of HZ contributes to the pathogenic effects of placental malaria. However, little is known about the direct impact of this crystal on placental tissue integrity. The present study aims to investigate the impact of nHZ and sHZ on human placental explants *in vitro*.

sHZ represents a valuable tool in malaria research due to its ability to mimic the structural and biological properties of nHZ. Several studies have demonstrated the utility of sHZ in elucidating mechanisms of host-parasite interactions [19]. For instance, sHZ has been used to study the activation of innate immune pathways, including Toll-like receptor 9 (TLR9)-mediated signaling [20]. Using sHZ offers several advantages over nHZ, including eliminating the need for parasite cultures, reducing experimental costs, and ensuring greater reproducibility in assays. Furthermore, minimizes the variability associated with nHZ, which may contain parasite-derived contaminants. These factors make sHZ a practical alternative for studying the biological effects of HZ.

2. Materials and methods

2.1. Culture of parasite and isolation of natural hemozoin

The FCB1 strain of *P. falciparum* was cultured in A+ erythrocytes up to 5–6 % parasitemia with mature stages predominant in culture, at 5 % hematocrit in RPMI medium supplemented with human serum as described previously [21]. The culture was checked weekly for *Mycoplasma* contamination by PCR. Natural HZ produced in cultures were isolated by exploiting its magnetic properties.

The *P. falciparum* cultures were centrifuged, and the pellet was washed once in RPMI medium and suspended at a hematocrit of ≈ 2–3 %. The RBC suspension was subjected to three cycles of freezing at −4°C and thawing at 37°C for 10 min each to lyse RBCs. The lysed RBC suspension was loaded onto an LS column (Miltenyi Biotec, Auburn, CA) and placed in the MACS separator. The magnetic field allowed the free HZ to be purified due to Hz retention [1]. The column was washed with PBS and removed from the magnetic field, and the HZ was eluted in distilled water and centrifuged at 4000 rpm. The supernatant was discarded, and the HZ precipitate was dried in an oven at 37°C until all moisture was eliminated. Once dry crystals were obtained, they were weighed, and working solutions were prepared at concentrations of 5 μg/mL and 10 μg/mL. These concentration choices for both nHZ and sHZ experiments were selected based on preliminary studies and relevant literature indicating that these concentrations are within the range where HZ is known to elicit measurable biological responses, such as immune activation or tissue interaction. These concentrations allow for the observation of clear effects without overwhelming the system, ensuring that the results are both significant and interpretable. Additionally, these levels are commonly used in similar experimental setups, providing consistency and comparability with other research in the field [22,23].

2.2. Synthesis of β-hematin

β-hematin or sHZ, was synthesized from hemin chloride at 60°C in an acetate buffer and was optimized based on a previous study [24]. The reaction was carried out by mixing hemin chloride with a sodium acetate buffer at pH 4.75. The mixture was stirred every 25 min for 5 min and maintained at 60°C for 3 h. Subsequently, the sample was allowed to settle, filtered, and washed three times with distilled water. Finally, the beta-hematin crystals were transferred to an incubator at 37°C for 48 h.

2.3. Characterization of nHZ and sHZ by scanning electron microscopy (SEM)

The samples were mounted on graphite tape and coated with a thin gold (Au) layer using a DENTON VACUUM Desk IV. They were then analyzed with a high-vacuum scanning electron microscope to obtain high-resolution images. A secondary electron detector was employed to assess the morphology and topography of the samples. SEM images were captured using a JEOL JSM-6490LV scanning electron microscope at magnifications of 20,000X and 25,000X. The average sizes of the β-hematin crystals were measured using ImageJ software.

2.4. Characterization of nHZ and sHZ by Fourier transform infrared spectroscopy (FTIR)

For FTIR analysis, the dehydrated sample, in powder form, was placed directly on the ATR crystal. Pressure was applied to ensure optimal contact between the sample and the crystal. Infrared light was

then directed through the crystal, and the reflected light was analyzed to obtain the infrared spectrum of the sample. The measurements were conducted at ambient temperature utilizing an IRTracer-100 infrared spectrometer (Shimadzu, Japan), employing 64 scans and a resolution covering a wavenumber range from 3500 to 400 cm-1.

2.5. Obtaining and culture of human placental explants

The study included 3 placentas from four-term pregnancies (gestation age ≥ 37 weeks). The placentas were donated by women between the ages of 23–33 who did not have any complications or health problems related to their pregnancy and deliver by cesarean section as per medical advice. The exclusion criteria for the study were as follows: for the mother, evidence or diagnosis of preeclampsia, diabetes mellitus, intrauterine infection, or any inflammatory process during pregnancy and delivery; for the fetus, the presence of intrauterine growth restriction or being small for gestational age. The pregnant women who donated their placenta signed the informed consent approved by the Ethics Committee of the Faculty of Medicine at the University of Antioquia (Minutes No. 015, 24/09/2020).

Placental tissue was collected under sterile conditions and processed within two hours after delivery. Using a scalpel, around six fragments of cotyledons were obtained, each measuring 1 × 2 cm and spanning the thickness of the placenta (3 cm) between the edges and the cord. These fragments were then dissected into approximately 0.5 cm^3 dimensions and placed in a well containing 3 mL of complete F-12 medium supplemented with 10 % fetal bovine serum and 1 % antibiotic. Two or three fragments were sowed per well, and the EPH culture was maintained for up to 72 h with daily medium change. The supernatant was collected daily during this period to determine lactate dehydrogenase (LDH) activity and human chorionic gonadotropin (hCG) production [25].

2.5.1. Exposure of human placental explants to nHZ and sHZ

All placental explants were washed three times with warm PBS 1X before treatment; for each placenta, five conditions were tested for 24 h: HPEs in culture medium (Control), HPEs exposed to 5 μg/mL and ten μg/mL of nHZ, HPEs exposed to 5 μg/mL and ten μg/mL of sHZ. After incubation, supernatants were collected for LDH, hCG, and cytokines measurements. A portion of the tissue was stored in 10 % formalin for routine histological analysis with hematoxylin and eosin staining (H&E), Cytokeratin 7 (CK-7), histochemical analysis of collagen distribution using Picro Sirius Red staining, and TUNEL staining. Finally, another portion of the tissue was preserved in Trizol for RNA extraction by qPCR. A total of 3 placentas were used in this study, and three replicates were performed on each placenta in each experiment.

2.6. Measurement of viability through Lactate Dehydrogenase (LDH) activity detection

Explant viability was evaluated by releasing the enzyme lactate dehydrogenase (LDH) into the incubation medium. LDH is an intracellular enzyme. Thus, their release reflects cytotoxicity. Following the manufacturer's recommendations, the LDH enzyme activity was assessed using the "Cytotoxicity detection kit" (Roche Diagnostics GmbH, Mannheim, Germany). After 24 h of HPE culture and coculture with nIE and *P. falciparum*-IE, Triton X-lysed tissue was employed as a positive control, representing 100 % LDH release.

2.7. Quantification of the hormone human gonadotropin chorionic (βhCG) in HPE supernatant

Concentrations of βhCG in culture supernatants of HPEs were determined by enzyme-linked immunosorbent assay (ELISA), using "DuoSet® ELISA kits" (R&D Systems) according to the manufacturer's instructions. Samples were added without further dilution. The absorbances were read at the Multiskan™ FC Microplate Photometer at 450 nm, and the concentration of βhCG was determined in pg/mL by extrapolating the data from the absorbance against a standard curve, normalized for every 100 μg of tissue. The assay sensitivity limits of the kits are 7.81 pg/mL to βhCG.

2.8. Histological and immunohistochemistry techniques

Placental explants were fixed in 10 % formaldehyde in 0.1 M phosphate buffer (pH 7.3) for 24 h, dehydrated in alcohol, clarified in xylene, embedded in paraffin, and sectioned at five μm. Paraffin histological sections were stained with hematoxylin-eosin (H&E) for routine histological analysis to evaluate the integrity of HPEs and quantify the presence of syncytial nodules, fibrin deposits, and infarction. For semi-quantitative analysis, collagen organization in HPE stroma was assessed using Sirius Red Picric (PSR) staining. To quantify the findings evaluated in H&E, ten random fields from each sample were chosen, and the frequency of HPEs with the parameter evaluated was determined. Histopathological damage scores in H&E sections and collagen histochemistry with PSR were assessed according to established histopathological scoring principles for research, as previously described [25,26]. see in Table 1**,** adapted from [27]. The slides were examined under light microscopy (Motic BA 310) at 40X magnification (total magnification = 400) with H&E and PSR at 20X magnification (total magnification = 200). The photos were taken with the Motic Images Plus 2.0 program.

For immunohistochemical analysis, tissue samples were deparaffinated with alcohol and xylene, and antigen retrieval was achieved by steaming the samples in sodium citrate buffer for 30 min. An anti-CK-7 antibody was added to assess the integrity of the trophoblast, followed by a secondary peroxidase-conjugated antibody. The antigen-antibody complex was visualized using DAB chromogen, and Mayer's hematoxylin provided nuclear contrast. A negative control was established using phosphate buffer instead of the primary antibody. Ten random fields from each sample were selected to determine the frequencies of the studied variables, including trophoblast detachment, trophoblast rupture, and villi denudation. The slides were examined under light microscopy (Motic BA 310) at 40X magnification (total magnification = 400), and the photos were taken with the Motic Images Plus 2.0 program. Following the methodology described previously [25].

2.9. Apoptosis assessment using the TUNEL assay

The DeadEnd™ Fluorometric TUNEL System was used to measure the number of apoptotic cells in HPE samples. This system detects fragmented DNA in apoptotic cells by catalytically incorporating fluorescein-12-dUTP at the DNA ends using the recombinant terminal deoxynucleotidyl transferase (rTdT) enzyme [28]. Samples were prepared by cutting 3-micron tissue sections from paraffin blocks, followed by formaldehyde treatment and staining according to the manufacturer's recommendations (Promega). Green fluorescence was employed to identify apoptotic cells, while DAPI staining served as a blue

Table 1
Scores for the analysis of the histopathological damage and Organization of collagen I.

Score	Histopathological damage	Organization of collagen I
1	Trophoblast/Fetal connective tissue intact	Absence of collagen birefringence
2	Minor detachment of the trophoblast and disorganization of fetal connective tissue	Low collagen birefringence
3	Almost complete detachment of trophoblast and disorganization of fetal connective tissue	Moderate collagen birefringence
4	Complete detachment of the trophoblast/ disorganization or destruction of fetal connective tissue	Strong collagen birefringence

background. A positive apoptosis control was utilized, involving HPEs treated with TNF-α for 24 h.

2.10. Statistical analysis

Data were presented as the mean ± standard error of the mean (SEM). LDH, hCG, and cytokines levels in culture supernatants of placental explants were normalized to tissue wet weight. The normality of the data was assessed using the Shapiro-Wilk statistical test, and repeated measures ANOVA was preferred because it allows for the analysis of data collected from the same subjects across multiple conditions or time points, accounting for intra-subject correlation and reducing variability. A *p-value* < 0.05 was considered statistically significant. The Tukey post hoc test was applied to compare different conditions. Graphs and statistical analyses were performed using GraphPad Prism version 10 (GraphPad Software, LLC. Boston, MA).

3. Results

3.1. Morphological and vibrational characterization of nHZ and sHz

nHZ and sHZ crystals were characterized by scanning electron microscopy (SEM) and infrared spectroscopy (IR). The analysis reveals that nHZ crystals exhibit a needle-like morphology, with approximate measurements of 500 nm (Fig. 1). This morphology aligns with findings from previous studies [29]. The micrograph of the natural sample shows a higher presence of crystalline aggregates, as previously documented [30]. Synthetic HZ showed a more evident distribution of crystals, which was achievable by the controlled scenario of synthesis (specific pH and temperature conditions).

The Fourier transform infrared spectroscopy (FTIR) of hemin, a structural component of hemoglobin, displays a firm band around 1695 cm^{-1}, corresponding to the carbonyl functional group (C═O) vibration in the porphyrin. On the other hand, the infrared spectrum of HZ shows three distinct bands associated with carbonyl groups, located approximately at 1205 cm^{-1}, 1655 $cm\text{-}^{1}$, and 1710 $cm\text{-}^{1}$. These bands indicate the formation of sHZ dimer (β-hematin). The provided figure confirms that the obtained crystals correspond to nHZ. The presence of these bands in the infrared spectrum supports the precise identification of HZ in the study (Fig. 2).

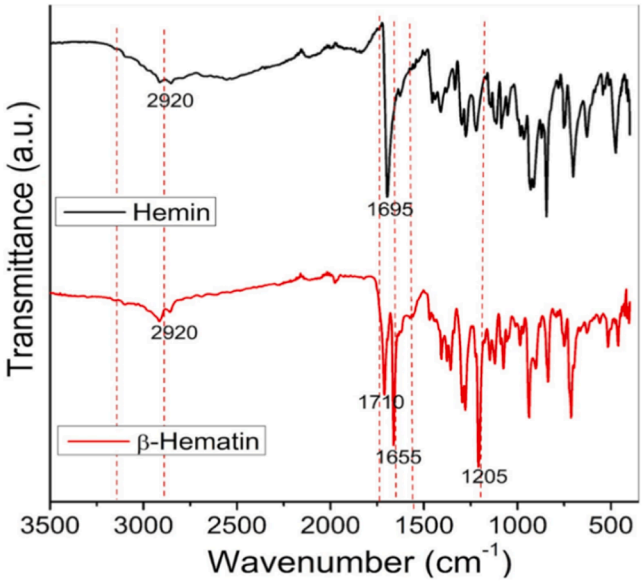

Fig. 2. FTIR of hemin and sHZ. The spectrum in the upper part (black lines) corresponds to hemin chloride, the reagent, and the spectrum in the lower part (red lines) corresponds to synthesized β-hematin. The formation of new bands is observed, confirming the synthesis of β-hematin.

3.2. LDH activity and βhCG production in HPEs exposed to natural and synthetic hemozoin ex vivo

The viability of the placental villi exposed to nHZ and sHZ was assessed by estimation of LDH activity and β-hCG concentrations in the supernatant cell culture after 24 h of treatment. LDH activity was used as an indicator of cell membrane integrity and, thus, a measurement of cytotoxicity. LDH activity was similar in all conditions studied, suggesting that neither nHZ nor sHZ have a cytotoxic effect on the tissue, and the results are comparable to the control group (Fig. 3A). The endocrine function of HPEs was evaluated by quantifying the production of hCG. HPEs exposed to both nHZ and sHZ showed a dose-dependent decrease in hCG production compared to the control group. However, no statistically significant differences were found (Fig. 3B). In the control group, the average of hCG was 709,6 pg/mL, and after treatment with 5 μg/mL of nHZ and sHz, the production reduced to 274 pg/mL and 336 pg/mL, respectively. When HPEs were treated with 10 μg/mL of nHZ and sHz, further reduction was observed, with levels dropping to 162 pg/mL and 88 pg/mL, respectively.

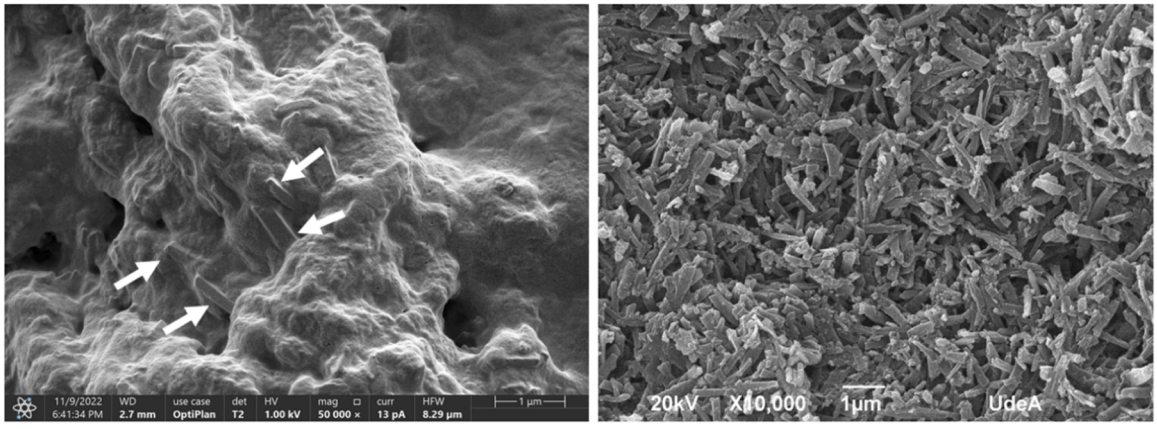

Fig. 1. Morphological characterization of natural hemozoin and synthetic. a. Scanning electron microscopy micrograph of nHZ crystals separated from *P. falciparum*-IE by magnetic column. The heme group dimerizes, forming a HZ dimer that constitutes triclinic needle-shaped structures (white arrow). These HZ dimers grow together through hydrogen bridges, creating long chains of hydrogen bonds that shape the various crystal terraces of HZ (black arrow). b. Scanning electron microscopy micrograph of sHZ shows a homogeneous distribution of crystals with a morphology like HZ.

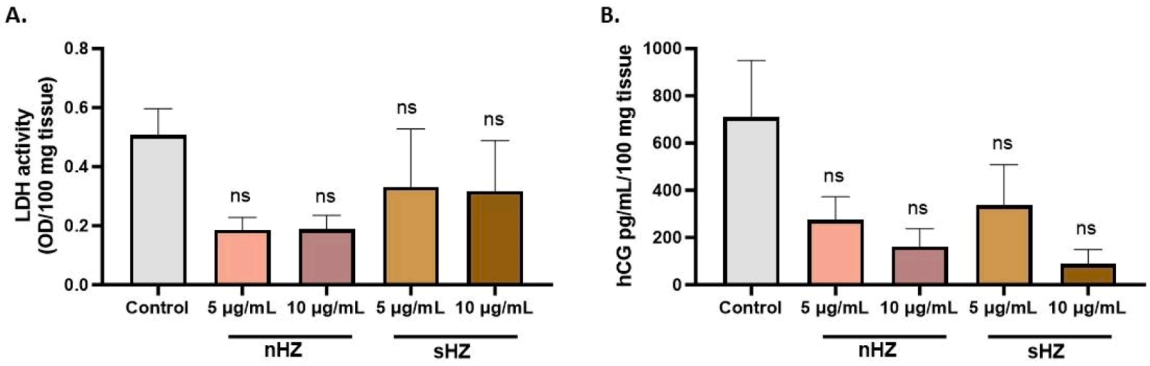

Fig. 3. LDH activity and βhCG production in HPEs exposed to nHZ and sHZ *ex vivo*. A. LDH activity was measured in the supernatant of HPEs as a marker of cytotoxicity, normalized per 100 mg of tissue. B. Production of βhCG measured in the supernatant of HPEs, normalized per 100 mg of tissue, in the study groups. Bar graphs represent the means ± SEM. Each symbol represents an individual donor ($n = 4$). One-way ANOVA to repeated measures with a test to multiple comparisons (Tukey test).

3.2.1. Hemozoin induces disorganization of placental villi and disruption of trophoblast

Histological analysis with H&E staining was performed on human placental explants exposed to two concentrations (5 µg/mL and 10 µg/mL) of nHZ and sHZ. Fig. 4 shows representative microphotographs of placental villi after exposition to HZ; both concentrations showed detachment of the trophoblast and fetal connective tissue disorganization. A histopathological damage score was calculated to provide a comprehensive overview of tissue damage based on trophoblast attachment to the villi and stroma organization. The score of the histopathological damage increased from 1.34 ± 0.15 in the control group to 3.17 ± 0.49 and 2.65 ± 0.39 in the tissue exposed to 10 µg/mL of nHZ and sHZ respectively (Fig. 4, *p-value* < 0.001).

The percentage of villi presenting pathological alterations such us syncytial knots, fibrin deposits, and infarction was also calculated and was similar in all conditions (data not presented), suggesting that either nHZ or sHZ has an impact mainly on the trophoblast attachment. Analysis using CK-7 immunohistochemistry, a specific marker of trophoblast, confirmed that ten µg/mL of nHZ and sHZ significantly disrupted the trophoblast layer of the placental villi (Fig. 4). Detachment and denudation of the trophoblast were predominantly observed.

A qualitative assessment of the distribution of type IV collagen was conducted using TCM. An increase in collagen fiber-deprived areas was observed in the villous stroma of HPEs exposed to both nHz and sHz, compared to non-exposed control HPEs, where fibers were regularly observed covering the villous stroma. Additionally, a semiquantitative evaluation of the distribution of type I collagen on the villous stroma was performed using PRS staining. It was found disorganization of collagen I in placental explants exposed to both concentrations of nHZ and sHZ, compared to the control samples, evidenced by a reduction in the

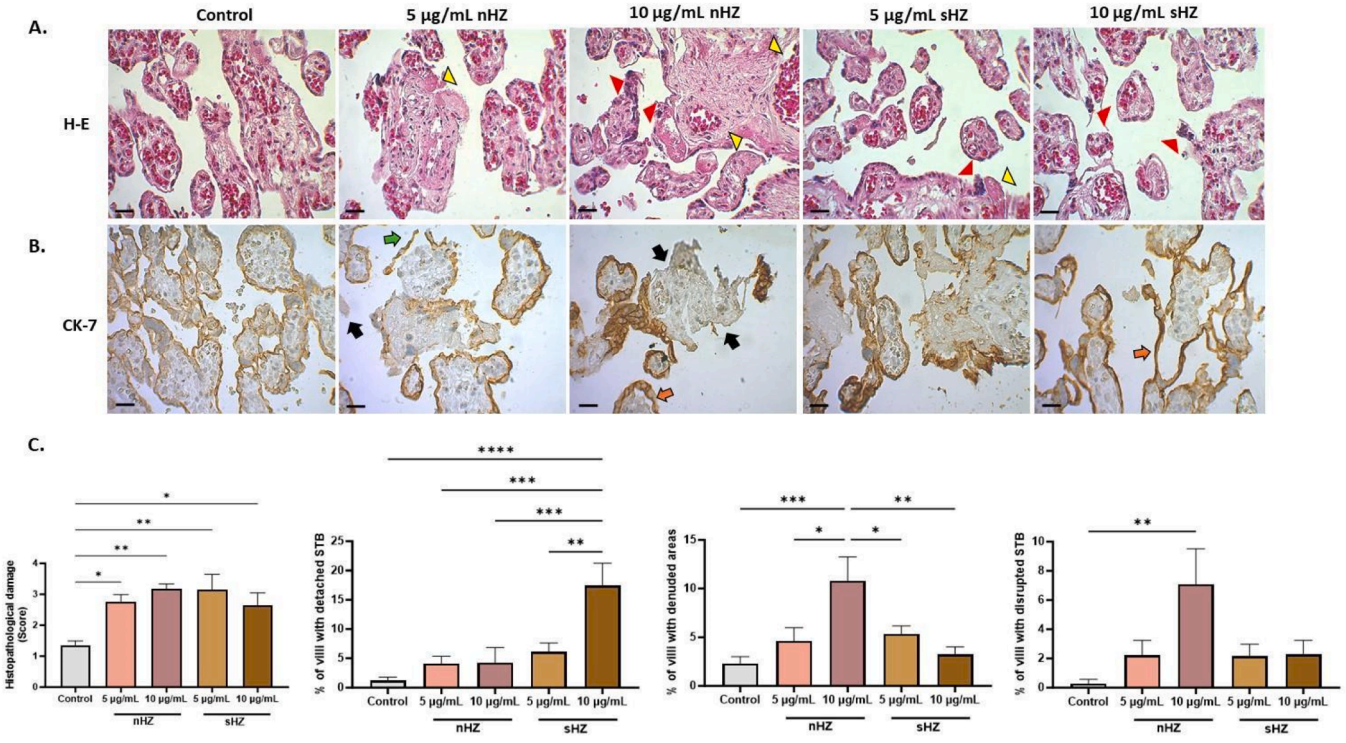

Fig. 4. Natural and synthetic hemozoin increases histological damage in *ex vivo*-exposed human placental explants. A. Panel of representative microphotographs of HPEs stained with H-E. Fibrin deposits (yellow arrowhead) and syncytial knots (red arrowhead) are shown. B. Panel of representative microphotographs of HPEs stained with CK-7. Detachment (orange arrows), denudation (black arrows), and rupture (green arrows) are shown. **C.** Results are presented as mean ± SEM ($n = 3$). Test: ANOVA, *p-value*: < 0.00001 (****), < 0.0001 (***), < 0.001 (**), < 0.05 (*). Scale bar: 20 µm. Total magnification 200X.

staining refringence (Fig. 5A) and the collage disorganization score (Fig. 5B).

3.2.2. *Hemozoin increases cellular apoptosis in human placental explants*

A notable increase in cellular apoptosis (cells in green fluorescence) was observed when HPEs were exposed to nHZ and sHZ. This phenomenon suggests a dose-dependent pattern: as HPEs were exposed to higher concentrations of HZ (10 μg/mL), cellular death increased (Fig. 6).

4. Discussion

Hemozoin, a pigment generated by *P. falciparum* during the digestion of hemoglobin in red blood cells, has emerged as a significant factor in the pathogenesis of malaria, particularly in its impact on the placenta, where it has been found not only free in the villous stroma but also phagocytized by leukocytes [12]. The results of this study demonstrate that HZ exacerbates the detachment and denudation of STB covering the placental villi. Additionally, disorganization of type I collagen fibers was observed, a crucial component for maintaining extracellular matrix integrity, indicating a role in the deterioration of placental tissue. However, the lack of variation in LDH activity across different conditions suggests that while structural damage occurs, cellular viability remains intact. This contrasts with the effects observed with the complete parasite, which significantly impacts cellular viability as indicated by previous studies [31].

Although cell viability, as assessed by LDH levels, was not affected, a significant increase in cellular apoptosis was observed. This discrepancy could be addressed by analyzing LDH levels after 48 or 72 h, along with conducting viability assessments using MTS, MTT, or ATP-based assays. This result can be explained by the fact that apoptosis leads to cell death in a controlled manner without immediately compromising overall cellular integrity, as measured by LDH.

LDH measures cell membrane damage and leakage, which may not be as evident in apoptotic cells, as they undergo a regulated process of cell death that does not necessarily cause immediate membrane rupture. Therefore, an increase in apoptosis can occur without a corresponding immediate rise in LDH levels. In this sense, it is more accurate to discuss apoptotic processes induced by HZ in placental tissue rather than necrotic processes, which are more associated with the complete parasite as previously reported [32]. It is important to mention that the apoptotic process is a normal or physiological process that should occur during placental development, involving cellular differentiation. This explains why apoptotic cells are also observed in control tissues or those not exposed to erythrocytes infected with *P. falciparum*, although in smaller proportions.

This finding aligns with observations from other studies that report similar effects on cellular apoptosis caused by HZ or parasite components, such as the heme group released during the lysis of infected cells [11]. These observations suggest that different mechanisms involving the parasite and HZ deposits may exert distinct effects on cellular viability or death, indicating that these processes may not be exclusive to a single component of the parasite or a single pathway. Additional parasitic products to consider in the pathophysiological process include parasite histone-DNA complexes and unbound glycosylphosphatidylinositol (GPI) anchors, which are also released into the circulation during schizont rupture [33–35]. It is noteworthy that both nHZ and sHZ showed a similar trend in the observed effects on both structural damage and apoptosis. This suggests a potential role for sHZ in biological assays that do not require special infrastructure and extensive laboratory work to obtain parasitic cultures with high densities, from which nHZ is derived. This sHZ synthesis process was described in detail previously [36].

Hemozoin deposits are often correlated with the severity of the disease in patients infected with *P. falciparum* [37,38]. In specific organ complications, such as cerebral malaria, it has been described those physiological concentrations of purified HZ are sufficient to be absorbed by central nervous system cells, alter the expression of pro-apoptotic proteins, and subsequently trigger apoptosis in human neurons and astrocytes [10]. This pro-apoptotic induction may also be accompanied by alterations in the cellular function of macrophages and leukocytes, leading to the release of a variety of pro-inflammatory mediators such as

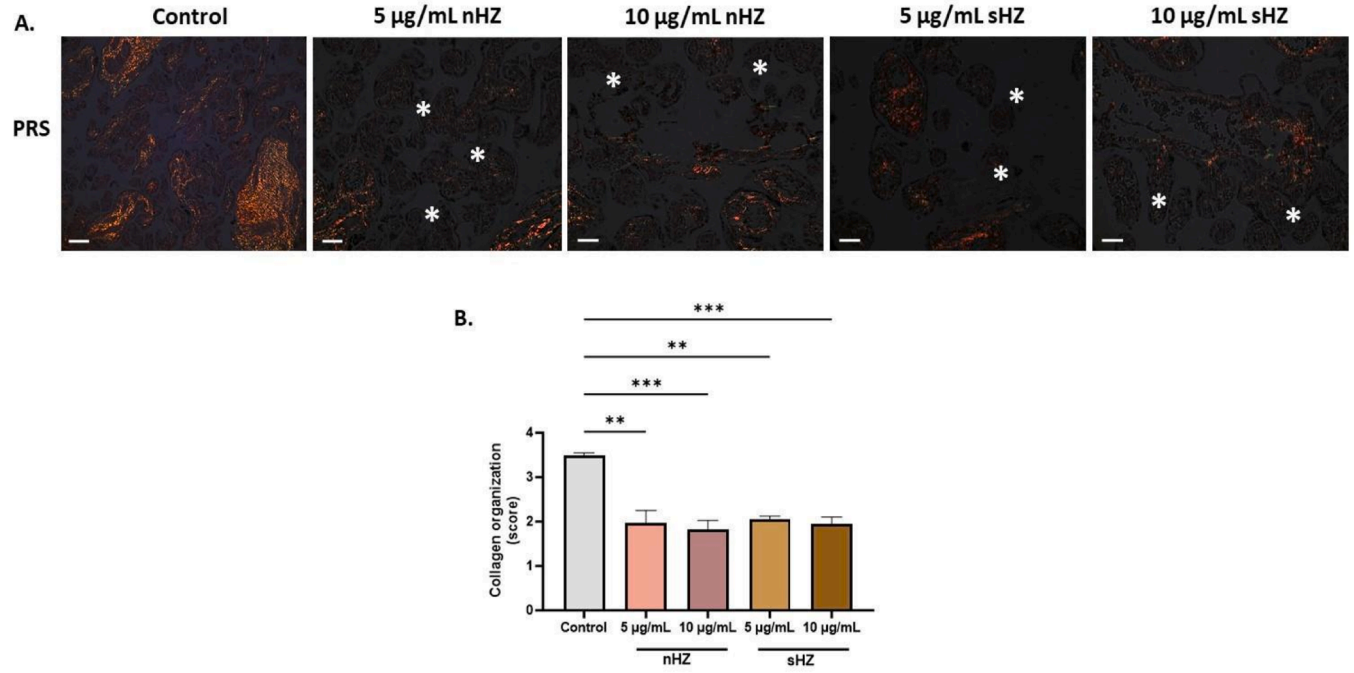

Fig. 5. Natural hemozoin disrupts the collagen distribution in the villous stroma of *ex vivo* exposed Human placental explants. A. Photographic panel of cross-sections of HPEs stained with PRS (orange staining of collagen fibers). Areas devoid of type I collagen fibers (white asterisk) are shown. B. Results are presented as mean ± SEM ($n = 3$). Test: ANOVA, *p-value*: < 0.0001 (***), < 0.001 (**). Scale bar: 20 μm. Total magnification 200X.

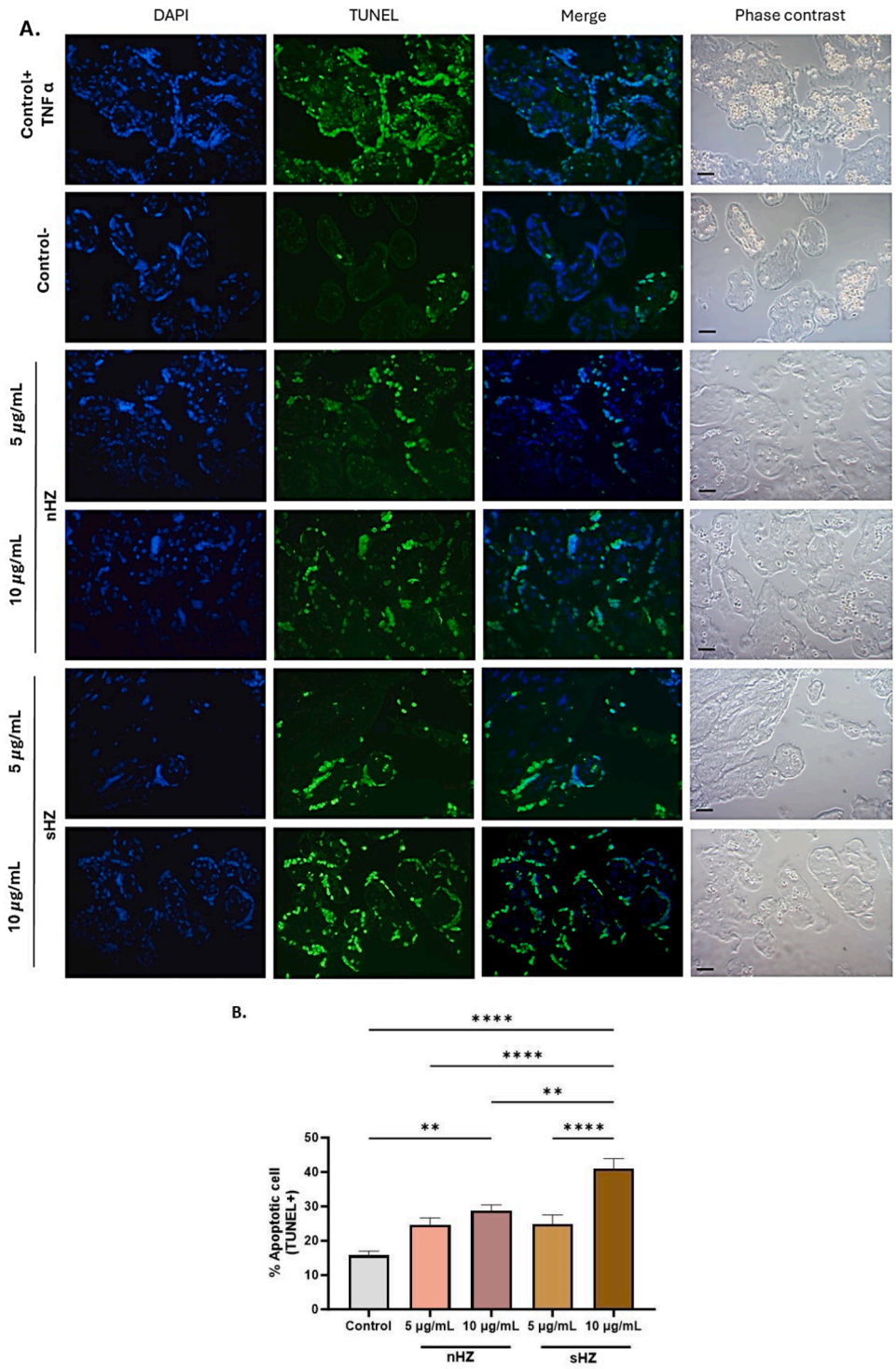

Fig. 6. Natural and synthetic hemozoin increases cellular apoptosis in *ex vivo* exposed human placental explants. A. Panel of representative photographs of HPEs exposed *ex vivo* to nHZ and sHZ labeled with TUNEL. The positive control consists of HPEs exposed to TNF-α (20 ng/mL) for 24 h, while the negative control consists of only HPEs. B. Frequency of the data presented in A. Bar graphs represent ME ± SEM. ($n = 3$). One-way repeated measures ANOVA with multiple comparisons Tukey test. Scale bar: 15 μm. Total magnification 400X.

TNF, MIF, MIPs, IL-1β, and IL-6 [39,40]. In this regard, the use of TNF as an apoptosis inducer in HPE control+ is further supported by this study.

In some infectious diseases, an increase in apoptosis in the placental tissue is also observed [41–45]. Specifically for the case of *Trypanosoma cruzi*, it has been described that apoptosis in the chorionic villi increases, reflected by an increase in the expression of markers such as M30, a neoepitope formed because of the cleavage of cytokeratin 18, in addition to inducing caspase-3-like activity in human chorionic villi [45]. These findings are suggested to be one of the mechanisms used by the parasite to ensure infection and invasion of the human placenta and fetus. These effects have also been correlated with alterations in the trophoblast, such as detachment and destruction of the trophoblast, as well as disorganization of the basal lamina and type I collagen in the placental trophoblast, very similar to what is observed in this study with HZ and to

what is observed with the complete *P. falciparum* parasite [31,46]. It is possible to hypothesize that HZ, like *T. cruzi*, could act on the activation of caspase-3 as an important mediator in the apoptotic process; this remains to be evaluated.

In the case of human cytomegalovirus (HCMV) infection in a primary trophoblast model, an increase in apoptosis and in the transcription factors and secretion of inflammatory cytokines, such as tumor necrosis factor-alpha (TNF-α) and interleukin-8, was observed. Interestingly, blocking TNF-α with a specific antibody inhibited the virus-induced apoptosis [42]. Also, infection of the trophoblast with HCMV has also been associated with TLR2 in STB [47]. The potential of TNF-α and Toll-like receptor pathways to induce apoptosis deserves evaluation in cases of malaria, particularly to assess the possible activation pathways that may induce apoptosis by the complete parasite or its derivatives. Cellular viability also reflects the damage caused by HCMV during trophoblast exposure; HCMV infection of villous trophoblasts results in the loss of up to half of the cultured cells within the first 24 h of exposure [47].

Toxoplasma gondii, for its part, has been described as inducing pyroptosis in human placental trophoblasts and amniotic cells through the induction of reactive oxygen species, which leads to the activation of the inflammasome [43]. A relevant process, as it has been described, is that among the possible innate resistance mechanisms available to villous trophoblasts is the induction of reactive oxygen species [48] and nitrogen intermediates [49]. The link between increased apoptosis in villous trophoblasts and placental pathologies, while seemingly obvious, is not fully understood. Most forms of villous pathology share the common feature of loss of the STB layer, which may be due to increased apoptosis and detachment of STB or a reduced capacity for CTB renewal. The loss of the STB barrier would allow access to the underlying fetal mesenchyme by progeny parasites or infected maternal leukocytes. Understanding the mechanism of this loss is crucial for understanding how *T. gondii* crosses the villous placenta [43].

In summary, each infectious agent, whether parasitic or viral, can potentially damage placental structure and may be related to the induction of shared pathways leading to cellular death or apoptosis, as well as structural damage to the placenta. It is crucial to note that the path to fully elucidate which routes are triggered by HZ to cause such significant damage is still long. However, it is promising to identify which processes are affected when the placenta is exposed solely to HZ without parasites. This is a reason to continue exploring these concepts with more specific assays to better target future treatments that could mitigate the adverse consequences of this infection.

The findings of this study could enable a more targeted approach in developing therapeutic interventions to mitigate the effects of placental malaria. For example, if it is confirmed that HZ plays a central role in placental dysfunction, more treatments could be developed that focus on blocking its accumulation or interaction with placental tissue cells, which would reduce inflammatory activation and associated apoptosis, ultimately improving pregnancy outcomes in women infected with *Plasmodium* spp [50].

Furthermore, research into the signaling pathways activated by HZ could lead to therapies that mitigate its inflammatory effects. For example, targeting Toll-like receptors (TLRs) [51], which recognize HZ, has shown promise in reducing inflammation and improving pregnancy outcomes in experimental models. These interventions could not only be helpful in the treatment of malaria during pregnancy but also for other pathological conditions related to inflammation and apoptosis, such as preeclampsia or autoimmune disorders [52]. In this regard, HZ could become a broader therapeutic target, offering a more comprehensive approach to managing obstetric complications associated with parasitic infections or inflammatory diseases.

5. Conclusion

Understanding the properties of HZ is crucial as it provides essential insights into its inherent structure, which is a fundamental aspect of malaria research. The increase in apoptosis observed in HPEs exposed to HZ supports the notion that HZ has a distinct effect on cellular death pathways compared to the complete parasite. This discrepancy suggests that HZ and other parasite components may act through different mechanisms, potentially involving distinct pathways of cellular viability and apoptosis. This information is valuable for further investigations concerning the interaction of HZ crystals with antimalarial agents, contributing to developing targeted therapeutic approaches against malaria. Furthermore, the similarity in morphology and size between the nHZ and sHZ suggests they might have comparable biological effects, as evidenced in the current study.

Further studies are required to determine the specific pathway through which HZ exerts its pathophysiological effect, which seems different from the complete parasite's effect. Future studies involving *in vivo* experiments, such as murine models, could provide additional information regarding the systemic immune response specifically triggered by HZ in placental tissue. However, it is crucial to consider the limitation that the murine placenta is morphologically very different from the human placenta, and the results obtained should take this factor into account in their interpretation.

CRediT authorship contribution statement

Urlike Kemmerling Weis: Writing – review & editing, Conceptualization. **Adriana Pabón:** Writing – review & editing, Conceptualization. **Ana María Vásquez:** Writing – review & editing, Methodology, Formal analysis, Data curation, Conceptualization. **Julieth Herrera:** Writing – original draft, Methodology, Investigation, Conceptualization, Formal analysis and Data curation of HZs . **Carolina Lopez Guzman:** Writing – original draft, Methodology, Investigation, Formal analysis, Data curation, Conceptualization. **Julián Zapata:** Writing – review & editing, Conceptualization.

Funding

This study was supported by Minciencias (Ministerio de Ciencia Tecnología e Innovación), Colombia, project code 111584467585, CT 921-2019, And CODI (Convocatoria programática 2019-2020: ciencias exactas y naturales, project code 2020-33176.

Declaration of Competing Interest

The authors declare no conflicts of interest.

Acknowledgments

Malaria Group of the University of Antioquia for providing the laboratory facilities to conduct these experiments. To "El laboratorio de Mecanismos de Infección Parasitaria" at the Institute of Biomedical Sciences, Faculty of Medicine, University of Chile, especially to its members Jesús Guerrero-Muñoz for assistance with placental tissue acquisition and TUNEL staining training, and Alejandro Fernández-Moya for support with histological staining. To Professors Cesar Augusto Barrero Meneses and Karen Edilma Garcia Tellez for guiding the synthetic production of β-hematin.

Informed Consent Statement

Informed consent was obtained from all subjects involved in the study. The study was conducted in accordance with the Declaration of Helsinki and approved by the ethics committee of the Faculty of Medicine at the University of Antioquia (Min No. 015, 09/24/2020) for studies involving humans.

Author contribution

This article was written by C.L.G, J.H., and A.M.V. A.M.V and C.L.G conceived the design of the study and the methodology approach, and analyzed the data. C.L.G and J.H. performed experiments and data collection. C.L.G., J.H., A.M.V., A.P., J. Z., and U.K.W reviewed, corrected, and approved the manuscript.

Data availability

Data will be made available on request.

References

[1] Biotec M. (2024, November). LS Columns, CA. MACS® Separator Starting Kits. Miltenyi Biotec. ⟨https://www.miltenyibiotec.com/⟩.
[2] WHO. World malaria report 2023. Geneva: World Health Organization; 2023.: Licence: CC BY-NC-SA 3.0 IGO.; 2023.
[3] Bannister LHS, I.W. *Plasmodium*. 2009.
[4] T.T. Pham, T.J. Lamb, K. Deroost, G. Opdenakker, P.E. Van den Steen, Hemozoin in malaria complications: more questions than answers, Trends Parasitol. 37 (3) (2021) 226–239.
[5] L.H. Miller, H.C. Ackerman, X.Z. Su, T.E. Wellems, Malaria biology and disease pathogenesis: insights for new treatments, Nat. Med 19 (2) (2013) 156–167.
[6] A. Rathi, Z. Chowdhry, A. Patel, et al., Hemozoin in malaria eradication—from material science, technology to field test, NPG Asia Mater. (2023).
[7] A.D. Sullivan, I. Ittarat, S.R. Meshnick, Patterns of hemozoin accumulation in tissue, Parasitology 112 (Pt 3) (1996) 285–294.
[8] T. Dalapati, J.M. Moore, Hemozoin: a complex molecule with complex activities, Curr. Clin. Microbiol Rep. 8 (2) (2021) 87–102.
[9] E.D. Guerra, F. Baakdah, E. Georges, D.S. Bohle, M. Cerruti, What is pure hemozoin? A close look at the surface of the malaria pigment, J. Inorg. Biochem 194 (2019) 214–222.
[10] E.A. Eugenin, J.A. Martiney, J.W. Berman, The malaria toxin hemozoin induces apoptosis in human neurons and astrocytes: potential role in the pathogenesis of cerebral malaria, Brain Res. 1720 (2019) 146317.
[11] M. Liu, S. Hassana, J.K. Stiles, Heme-mediated apoptosis and fusion damage in BeWo trophoblast cells, Sci. Rep. 6 (2016) 36193.
[12] R. McGready, A. Brockman, T. Cho, M.A. Levesque, A.N. Tkachuk, S.R. Meshnick, et al., Haemozoin as a marker of placental parasitization, Trans. R. Soc. Trop. Med. Hyg. 96 (6) (2002) 644–646.
[13] B.J. Brabin, C. Romagosa, S. Abdelgalil, C. Menéndez, F.H. Verhoeff, R. McGready, et al., The sick placenta-the role of malaria, Placenta 25 (5) (2004) 359–378.
[14] S.J. Rogerson, L. Hviid, P.E. Duffy, R.F. Leke, D.W. Taylor, Malaria in pregnancy: pathogenesis and immunity, Lancet Infect. Dis. 7 (2) (2007) 105–117.
[15] N.W. Lucchi, D. Sarr, S.O. Owino, S.M. Mwalimu, D.S. Peterson, J.M. Moore, Natural hemozoin stimulates syncytiotrophoblast to secrete chemokines and recruit peripheral blood mononuclear cells, Placenta 32 (8) (2011) 579–585.
[16] A.L. Suguitan, T.J. Cadigan, T.A. Nguyen, A. Zhou, R.J. Leke, S. Metenou, et al., Malaria-associated cytokine changes in the placenta of women with preterm deliveries in Yaounde, Cameroon, Am. J. Trop. Med. Hyg. 69 (6) (2003) 574–581.
[17] S.J. Rogerson, H.C. Brown, E. Pollina, E.T. Abrams, E. Tadesse, V.M. Lema, et al., Placental tumor necrosis factor alpha but not gamma interferon is associated with placental malaria and low birth weight in Malawian women, Infect. Immun. 71 (1) (2003) 267–270.
[18] A.J. Umbers, P. Boeuf, C. Clapham, D.I. Stanisic, F. Baiwog, I. Mueller, et al., Placental malaria-associated inflammation disturbs the insulin-like growth factor axis of fetal growth regulation, J. Infect. Dis. 203 (4) (2011) 561–569.
[19] M.S. Lee, Y. Igari, T. Tsukui, K.J. Ishii, C. Coban, Current status of synthetic hemozoin adjuvant: a preliminary safety evaluation, Vaccine 34 (18) (2016) 2055–2061.
[20] C. Coban, K.J. Ishii, T. Kawai, H. Hemmi, et al., Toll-like receptor 9 mediates innate immune activation by the malaria pigment hemozoin, J. Exp. Med. 201 (1) (2005) 19–25.
[21] A.M. Vásquez, C. Segura, S. Blair, Induction of pro-inflammatory response of the placental trophoblast by Plasmodium falciparum infected erythrocytes and TNF, Malar. J. 12 (2013) 421.
[22] J.H. Lee, H.R. Kim, J.H. Lee, et al., Enhanced in-vitro hemozoin polymerization by optimized process using histidine-rich protein II (HRP II), Polymers 11 (7) (2019) 1162.
[23] I.C. Hirako, M.M. Antunes, R.M. Rezende, et al., Uptake of Plasmodium chabaudi hemozoin drives Kupffer cell death and fuels superinfections, Sci. Rep. 12 (2022) 19805.
[24] J. Herrera, C. Parra, D. Coronado-Cardona, V. Perez, J. Zapata, et al., Revising the formation of β-hematin crystals from hemin in aqueous-acetate medium containing chloroquine: modeling the kinetics of crystallization and characterizing their physicochemical properties, Cryst. Growth Des. 23 (7) (2023) 4791–4806.
[25] C. López-Guzmán, A.M. García, P. Marín, A.M. Vásquez, Assessment of the integrity and function of human term placental explants in short-term culture, Methods Protoc. 7 (1) (2024).
[26] K.N. Gibson-Corley, A.K. Olivier, D.K. Meyerholz, Principles for valid histopathologic scoring in research, Vet. Pathol. 50 (6) (2013) 1007–1015.
[27] A. Liempi, C. Castillo, L. Medina, N. Galanti, J.D. Maya, V.H. Parraguez, et al., Comparative ex vivo infection with Trypanosoma cruzi and Toxoplasma gondii of human, canine and ovine placenta: analysis of tissue damage and infection efficiency, Parasitol. Int 76 (2020) 102065.
[28] Y. Gavrieli, Y. Sherman, S.A. Ben-Sasson, Identification of programmed cell death in situ via specific labeling of nuclear DNA fragmentation, J. Cell Biol. 119 (3) (1992) 493–501.
[29] C. Wendt, W. de Souza, A. Pinheiro, L. Silva, A.A. de Sa Pinheiro, R. Gauvin, K. Miranda, High-resolution electron microscopy analysis of malaria hemozoin crystals reveals new aspects of crystal growth and elemental composition, Cryst. Growth Des. 21 (10) (2021) 5521–5533.
[30] M. Boura, R. Frita, A. Góis, T. Carvalho, T. Hänscheid, The Hemozoin conundrum: Is malaria pigment immune activating, inhibiting, or simply a bystander? Trends Parasitol. 29 (10) (2013).
[31] C. López-Guzmán, A.M. García, J.D. Ramirez, T.T. Aliaga, A. Fernández-Moya, U. Kemmerling, et al., Plasmodium falciparum alters the trophoblastic barrier and stroma villi organization of human placental villi explants, Malar. J. 23 (1) (2024) 130.
[32] I.P. Crocker, O.M. Tanner, J.E. Myers, J.N. Bulmer, G. Walraven, P.N. Baker, Syncytiotrophoblast degradation and the pathophysiology of the malaria-infected placenta, Placenta 25 (4) (2004) 273–282.
[33] D.C. Gowda, TLR-mediated cell signaling by malaria GPIs, Trends Parasitol. 23 (12) (2007) 596–604.
[34] F.F. Dutra, M.T. Bozza, Heme on innate immunity and inflammation, Front. Pharm. 5 (2014) 115.
[35] M.R. Gillrie, K. Lee, D.C. Gowda, S.P. Davis, M. Monestier, L. Cui, et al., Plasmodium falciparum histones induce endothelial proinflammatory response and barrier dysfunction, Am. J. Pathol. 180 (3) (2012) 1028–1039.
[36] J.P.C. Herrera, D. Coronado, V. Perez, et al., Revising the formation of β-hematin crystals from hemin in aqueous-acetate medium containing chloroquine: modeling the kinetics of crystallization and characterizing their physicochemical properties, Cryst. Growth Des. (2023) 4791–4806.
[37] G.E. Grau, C.D. Mackenzie, R.A. Carr, M. Redard, G. Pizzolato, C. Allasia, et al., Platelet accumulation in brain microvessels in fatal pediatric cerebral malaria, J. Infect. Dis. 187 (3) (2003) 461–466.
[38] S. Maknitikul, N. Luplertlop, G.E.R. Grau, S. Ampawong, Dysregulation of pulmonary endothelial protein C receptor and thrombomodulin in severe falciparum malaria-associated ARDS relevant to hemozoin, PLoS One 12 (7) (2017) e0181674.
[39] B.A. Sherry, G. Alava, K.J. Tracey, J. Martiney, A. Cerami, A.F. Slater, Malaria-specific metabolite hemozoin mediates the release of several potent endogenous pyrogens (TNF, MIP-1 alpha, and MIP-1 beta) in vitro, and altered thermoregulation in vivo, J. Inflamm. 45 (2) (1995) 85–96.
[40] M. Jaramillo, M. Godbout, M. Olivier, Hemozoin induces macrophage chemokine expression through oxidative stress-dependent and -independent mechanisms, J. Immunol. 174 (1) (2005) 475–484.
[41] K. Bernischke PK, R.N. Baergen. Pathology of the human placenta. 2006. p. 1069.
[42] G. Chan, L.J. Guilbert, Ultraviolet-inactivated human cytomegalovirus induces placental syncytiotrophoblast apoptosis in a Toll-like receptor-2 and tumour necrosis factor-alpha dependent manner, J. Pathol. 210 (1) (2006) 111–120.
[43] M. Abbasi, K. Kowalewska-Grochowska, M.A. Bahar, R.T. Kilani, B. Winkler-Lowen, L.J. Guilbert, Infection of placental trophoblasts by Toxoplasma gondii, J. Infect. Dis. 188 (4) (2003) 608–616.
[44] Y. Li, Y. Shibata, L. Zhang, N. Kuboyama, Y. Abiko, Periodontal pathogen Aggregatibacter actinomycetemcomitans LPS induces mitochondria-dependent-apoptosis in human placental trophoblasts, Placenta 32 (1) (2011) 11–19.
[45] J. Duaso, G. Rojo, F. Jaña, N. Galanti, G. Cabrera, C. Bosco, et al., Trypanosoma cruzi induces apoptosis in ex vivo infected human chorionic villi, Placenta 32 (5) (2011) 356–361.
[46] J. Duaso, G. Rojo, G. Cabrera, N. Galanti, C. Bosco, J.D. Maya, et al., Trypanosoma cruzi induces tissue disorganization and destruction of chorionic villi in an ex vivo infection model of human placenta, Placenta 31 (8) (2010) 705–711.
[47] G. Chan, D.G. Hemmings, A.D. Yurochko, L.J. Guilbert, Human cytomegalovirus-caused damage to placental trophoblasts mediated by immediate-early gene-induced tumor necrosis factor-alpha, Am. J. Pathol. 161 (4) (2002) 1371–1381.
[48] D. Arsenijevic, H. Onuma, C. Pecqueur, S. Raimbault, B.S. Manning, B. Miroux, et al., Disruption of the uncoupling protein-2 gene in mice reveals a role in immunity and reactive oxygen species production, Nat. Genet. 26 (4) (2000) 435–439.
[49] S.C. Smith, L.J. Guilbert, J. Yui, P.N. Baker, S.T. Davidge, The role of reactive nitrogen/oxygen intermediates in cytokine-induced trophoblast apoptosis, Placenta 20 (4) (1999) 309–315.
[50] L.M. Coronado, C.T. Nadovich, C. Spadafora, Malarial hemozoin: from target to tool, Biochim. Biophys. Acta 1840 (6) (2014) 2032–2041.
[51] R. Barboza, F.A. Lima, A.S. Reis, et al., TLR4-mediated placental pathology and pregnancy outcome in experimental malaria, Sci. Rep. 7 (2017) 8623.
[52] L. Sharma, G. Shukla, Placental malaria: a new insight into pathophysiology, Front. Med. (Lausanne) 4 (2017) 117.